Nuclear Physics **A458** (1986) 217–224
North-Holland, Amsterdam

PHOTOFISSION OF ^{232}Th NEAR THRESHOLD

D.J.S. FINDLAY, N. P. HAWKES and M.R. SENÉ

Nuclear Physics Division, Harwell Laboratory, Oxon. OX11 0RA, England

Received 11 April 1986

Abstract: Measurements are presented of the photofission cross section and the mean number $\bar{\nu}$ of neutrons per fission for ^{232}Th made using bremsstrahlung from the Harwell electron linear accelerator HELIOS and a high efficiency neutron detector to record neutron multiplicity distributions. The cross section is interpreted in terms of a fission barrier with shallow wells in two separate outer barriers. Interesting structure is observed in $\bar{\nu}$ as a function of photon energy.

E NUCLEAR REACTIONS ^{232}Th (γ, F), $E = 5.5$–7 MeV; measured photon induced fission $\sigma(E)$; deduced average neutron number VSE. ^{232}Th deduced fission characteristics.

1. Introduction

The fission of thorium has been the subject of much research, both experimental and theoretical. Recently considerable attention has been focussed on resonances observed in thorium fission cross-section measurements near threshold which have been interpreted in terms of a shallow third well splitting the outer hump of the double humped fission barrier [1,2]). Many measurements have been made with neutrons using the even-even nuclei ^{230}Th and ^{232}Th as targets, producing odd mass systems with several open fission channels. However, if measurements are made using photons, then only a very few fission channels are involved, and indeed for ^{232}Th, experimental photofission angular distributions have shown that the $J^{\pi}K = 1^{-}0$ channel is predominant by at least an order of magnitude near threshold [3,4]). The predominance of one fission channel eases the interpretation of data.

There have been many previous photofission experiments on ^{232}Th. Experiments in the energy region near threshold include those performed with bremsstrahlung [4–7]), quasi-monochromatic photons from positron annihilation in flight [8,9]), variable energy Compton scattered gammas [10,11]), proton capture gammas [12]) and tagged photons [13,14]). In most experiments only the photofission cross section $\sigma_{\gamma f}$ was measured, usually by detecting the fission fragments. Only in the two experiments performed at Livermore [7–9]) was the mean number $\bar{\nu}$ of neutrons per fission measured, a quantity which can reflect the dynamics of the passage from saddle to scission. Further, in most experiments the photon energy resolution was insufficient to resolve any structure expected from a third well. The only experiment to unambiguously resolve such structure in the cross section was recently carried out by

Knowles *et al.* [14]) at Illinois and achieved the very good energy resolution of 14 keV. In the present experiment the photofission cross section $\sigma_{\gamma f}$ for ^{232}Th was measured with an energy resolution of 80 keV below 6.5 MeV, energy resolution worse than that of the recent Illinois experiment, but with better statistical precision of the cross-section datum points at lower photon energies. Furthermore, in the present experiment $\bar{\nu}$ was also measured, an energy resolution of 110 keV below 6.5 MeV being achieved.

The present measurements were made using bremsstrahlung, employing a new technique to ensure reliable results, and a high efficiency neutron detector to record multiplicity distributions of prompt neutrons from the ^{232}Th photonuclear target, enabling simultaneous measurements to be made of the photofission cross-section and $\bar{\nu}$.

2. Experimental method

The present measurements were made on the Low Energy beam line of the 136 MeV Harwell electron linear accelerator HELIOS [15]). The experimental arrangement is shown schematically in fig. 1. The electron beam from the first two sections of the eight section accelerator was energy analysed to ±0.5% by energy defining slits. The magnetic field in the bending magnets, stabilised by computer assisted feedback to ±0.05%, was measured using a Rawson–Lush rotating coil gaussmeter, and the energy scale was established by measuring the 6.191 MeV threshold of the ^{183}W(γ, n) reaction. Bremsstrahlung from a 0.10 g · cm^{-2} gold radiator, collimated to a solid angle of 0.043 msr, struck the ^{232}Th photonuclear target 4.5 m from the radiator. The bremsstrahlung dose was measured by an NBS-type P2 chamber beyond the phonuclear target. The target was surrounded by the neutron detector, a large oil moderated assembly of fifty-six $^{10}BF_3$ counters having an efficiency of 0.44 for fission neutrons [16,17]). The distribution of multiplicities of detected neutrons was recorded on a PDP-11/45 computer. The event rate was kept at ≤0.1 events per beam burst over the whole energy range by using ^{232}Th target thicknesses of between 2 mg · cm^{-2} and 4 g · cm^{-2} to ensure that distortion of the multiplicity distribution due to overlap* of distinct events could be reliably corrected.

In the present experiment the bremsstrahlung yield curve was measured in steps of only 50 keV below 6.5 MeV and 100 keV above 6.5 MeV. To minimise the effects of any shifts in the mean energy of the electron beam due to accelerator variations, a new measurement technique was employed. Since the cross section unfolded from a bremsstrahlung yield curve depends mostly on the differences between neighbouring points on the yield curve, these differences were arranged to be the primary measurements in the present experiment. During each difference measurement the

* An example of overlap is the detection of one neutron from one photofission reaction and the detection of a second neutron from a second reaction in the same beam burst. This appears indistinguishable from a multiplicity 2 event from a single reaction.

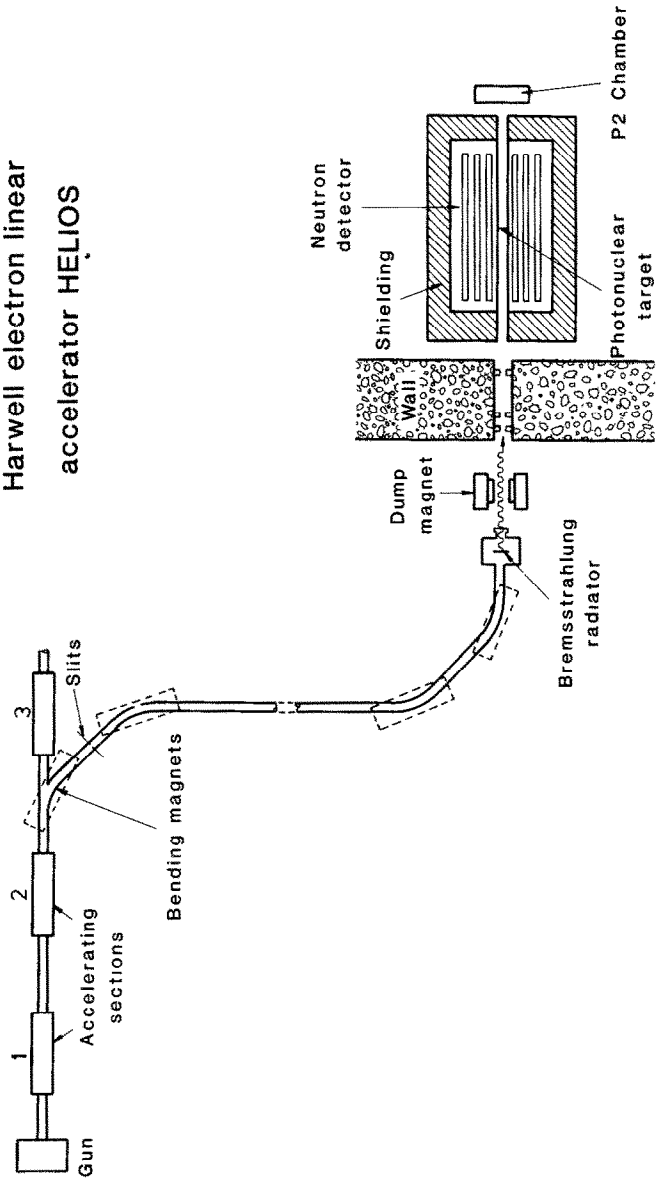

Fig. 1. The experimental arrangement used for the photofission measurements (not to scale).

electron beam energy was switched back and forth between two values 50 keV apart (100 keV above 6.5 MeV) by switching the magnetic field in the bending magnets comprising the first 90° bend of the beam transport system. The magnetic field was changed every minute, and two sets of data were recorded, one for each energy. Each yield difference measurement lasted ~2 hours below the photoneutron threshold (6.44 MeV) and ~8 hours above. Further details of the experimental technique may be found in ref. [18]).

3. Analysis

The raw data comprise the set of pairs of neutron multiplicity distributions corresponding to neighbouring bremsstrahlung endpoint energies. All distributions were corrected for background, dead-time and overlap according to ref. [16]), and the lower energy distribution of each pair was then subtracted from its partner to give a set of difference distributions. This set of distributions was then regarded as a set of yield difference curves, one for each multiplicity, and these curves were separately unfolded to give cross sections for each multiplicity as a function of photon energy. The bremsstrahlung spectrum in the present experiment was calculated using a method [19]) based on partial wave calculations of the bremsstrahlung integrated-over-angle cross section and including the angular distribution of the bremsstrahlung cross section, electron energy losses in the bremsstrahlung radiator and the energy spectrum of the electron beam incident on the radiator. The unfolding was carried out using the method of ref. [20]) recast in terms of yield differences. This unfolding method is a modification to the Penfold–Leiss unfolding method which specifically accommodates the detailed behaviour of the bremsstrahlung spectrum near the endpoint. The effective photon energy spectrum for the unfolded cross-section datum points, constructed from a suitable linear combination of bremsstrahlung spectra at different endpoint energies, is typically as shown in fig. 2; the width of the resolution function (fwhm) can be seen to be 80 keV. The final stage in the data analysis was to fit the cross sections for individual multiplicities at the same photon energies with the TRDG neutron multiplicity distribution [21]) to obtain the number of fissions and hence $\sigma_{\gamma f}$ and $\bar{\nu}$. The TRDG distribution is an extension of the popular Terrell neutron multiplicity distribution to accommodate separate consideration of the two fission fragments, and has been shown [21]) to substantially improve the fit to multiplicity distributions. Below the photoneutron threshold all multiplicities were fitted, but above only multiplicities greater than or equal to 2 were fitted.

4. Results and discussion

The photofission cross section for ^{232}Th measured in the present experiment is shown in fig. 3. The errors shown are statistical, and in addition there is an overall systematic error of ~10%. The photon energy resolution (fwhm) is 80 keV below

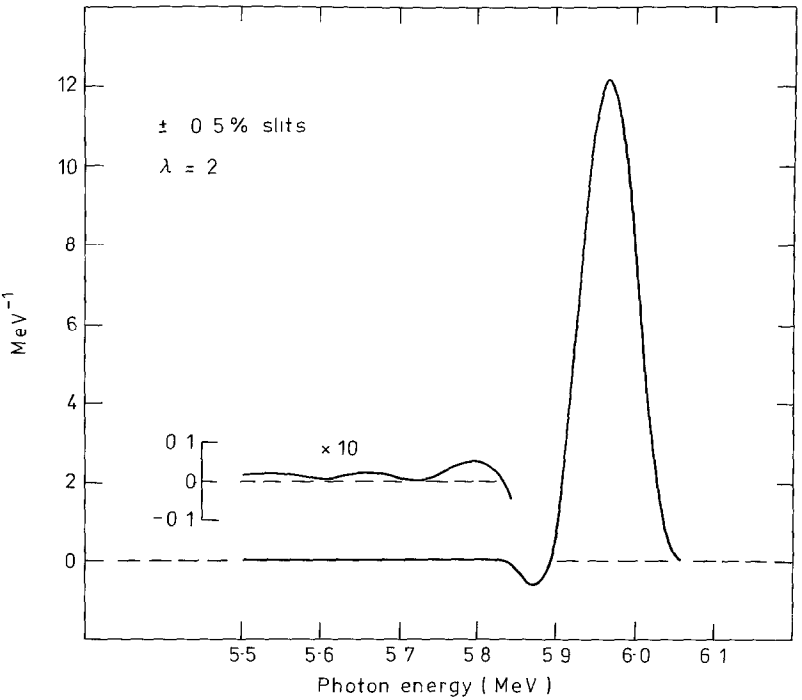

Fig. 2. Typical effective photon energy spectrum (resolution function) for unfolded cross-section datum points. [The parameter λ is used as described in ref. [20]) to produce a suitable compromise between the width of the main peak and oscillations in the tail.]

6.5 MeV and 200 keV above 6.5 MeV. There is one plateau between about 5.40 and 5.75 MeV where a pair of peaks is evident (at 5.47 and 5.62 MeV), and there is a second plateau between about 5.90 and 6.10 MeV where there is evidence for a second pair of resonances (there is a shoulder at 5.92 MeV and a peak at 6.02 MeV). Also shown are the data of Knowles *et al.* [14]) measured at Illinois with 14 keV photon energy resolution. The present measurements confirm the resonances in the Illinois data except for their peak at 5.70 MeV which is not evident in the present data, and also confirm that the fall in the fission cross section which begins about 6.35 MeV is unrelated to the onset of neutron emission at 6.44 MeV. The present data agree, in general, very well with the Illinois data. Although the nominal energy resolution in the Illinois experiment is 14 keV, the statistical precision of the individual datum points of the cross section is not high at lower photon energies and so the usefulness of this energy resolution is reduced. At lower photon energies the present data may offer a more useful combination of energy resolution and statistical precision.

The values for $\bar{\nu}$ are shown in fig. 4. Here the photon energy resolution is 110 keV below 6.5 MeV, 200 keV between 6.5 and 6.6 MeV and 390 keV above 6.6 MeV. There is structure below the photoneutron threshold and a negative slope between about

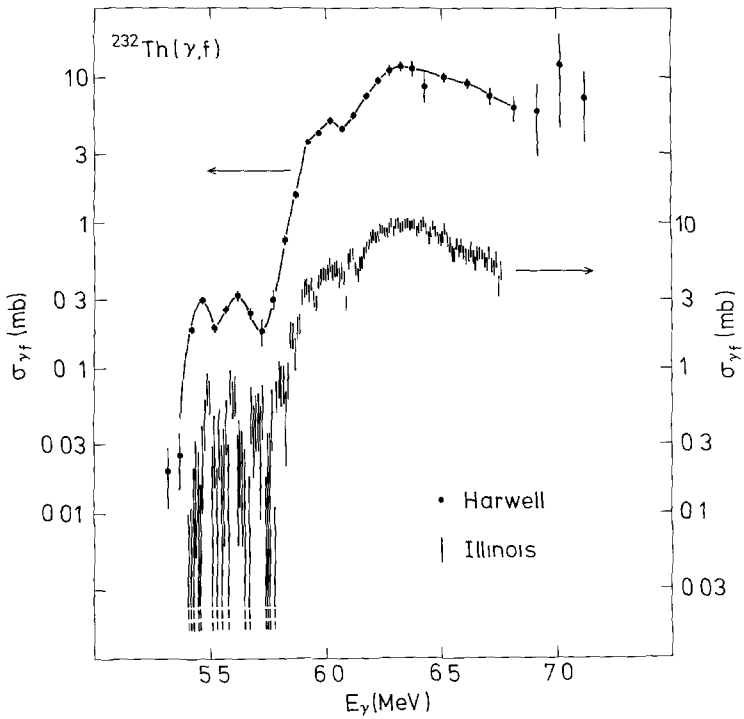

Fig. 3. The photofission cross section $\sigma_{\gamma f}$ for ^{232}Th. Solid circles, present data; lines, data from ref. [14]). Note that the sets of data are displaced by a factor 10. The solid line serves only to guide the eye.

6 and 7 MeV. The only previous $^{232}Th(\gamma, f)$ $\bar{\nu}$ measurements were made at Livermore using bremsstrahlung [7]), and then in more detail using quasi-monochromatic photons from positron annihilation [9]) with an energy resolution of ~300 keV. The latter data, also shown in fig. 4, suggest a negative slope between about 6 and 8 MeV, but are systematically lower than the present values. Part of this difference is due to the use of the Terrell multiplicity distribution in the Livermore analysis, since fitting a Terrell distribution is known [21]) to underestimate $\bar{\nu}$ by ~0.1 for $\bar{\nu} = 2$.

The dependence of $\bar{\nu}$ on energy in fig. 4 is clearly very different from the approximately linear increase with the excitation energy of the fissioning system observed in other actinides. Making the usual assumption that the numbers of neutrons emitted from primary fission fragments increase as their excitation energies increase, the present results show that, at least up to ~7 MeV, increases in the excitation energy of the fissioning system do not appear as increases in the excitation energies of the fission fragments. The ^{232}Th nucleus appears to be the nucleus for which $\bar{\nu}$ fails to increase with excitation energy over the widest energy range. This is consistent with the $^{232}Th(\alpha, \alpha' f)$ measurements of David *et al.* [22]) which show that below ~8 MeV an increase ΔE in the excitation energy of the ^{232}Th fissioning system produces an increase $\geqslant \Delta E$ in the kinetic energy of the fission fragments, although

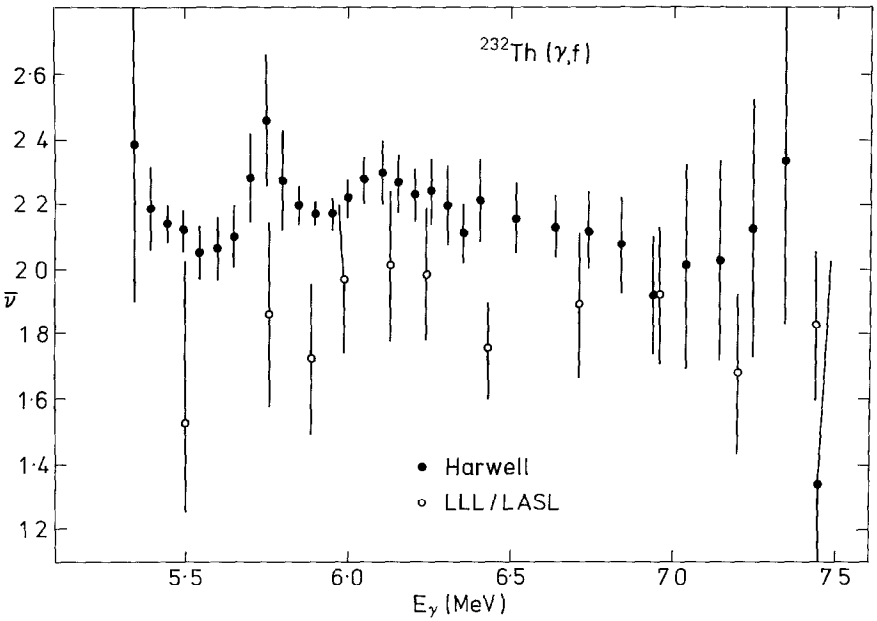

Fig. 4. The mean number $\bar{\nu}$ of neutrons per fission for ^{232}Th. Solid circles, present data; crosses, data from ref. [9]).

the comparison is not rigorous because of the different fission channels involved in photofission and alpha-induced fission.

Structure of the kind observed in the present $\bar{\nu}$ data has been interpreted [23]) in the case of the $^{232}Th(n, f)$ reaction in terms of variations in the division of reaction strength amongst different fission channels. However this interpretation is unlikely to be valid for the present ^{232}Th data since one fission channel, $J^{\pi}K = 1^{-}0$, predominates by at least an order of magnitude. The structure in the present $\bar{\nu}$ values may reflect structure in the surface describing the variation of potential energy of the fissioning system with deformation; the presence of such structure in the surface means that different excitation energies could produce different scission configurations which would in turn lead to different values of $\bar{\nu}$. Such an explanation could be confirmed by measurement of the mass distribution of fission fragments from the photofission of thorium as a function of photon energy in this energy region.

Either of the two pairs of resonances in the photofission cross section in fig. 3 could be interpreted as resonances in a shallow third well. But the presence of two plateaus in the cross section, each having a pair of resonances on it, and each corresponding to different average values of $\bar{\nu}$ as shown in fig. 4, suggests a more complicated explanation. A recent calculation [24]) of the potential energy surface for the fission of ^{232}Th, using a spin orbit potential for the shell corrections which was chosen specifically to fit measured nuclear properties at high deformations, predicted two saddles at deformations corresponding to the outer hump of the double humped

fission barrier. In this calculation only symmetric deformations were considered, but it is not improbable that the inclusion of asymmetric deformations would lead to the appearance of splits in these saddles producing a shallow well near the top of each. The two saddles are predicted to be ~300 keV apart, which is similar to the separation of the pairs of resonances in the present measurement. The two pairs of resonances in the cross section would then be resonances in the two different shallow wells, and the corresponding different average $\bar{\nu}$ values would be due to fission over the higher saddle leading to scission configurations in which, on average, the primary fission fragments evaporate slightly more neutrons.

5. Conclusions

This paper has reported new measurements of $\sigma_{\gamma f}$ and $\bar{\nu}$ for the photofission of ^{232}Th with photon energy resolutions $\lesssim 100$ keV. Structure in both $\sigma_{\gamma f}$ and $\bar{\nu}$ suggests that the potential energy surface of the fissioning system is a complex function of both deformation and excitation energy, particularly in the region of the outer hump, and highlights the need for further theoretical work on this problem.

Work described in this paper was undertaken as part of the Underlying Research Programme of the UKAEA.

References

1) S. Bjørnholm and J.E. Lynn, Rev. Mod. Phys. **52** (1980) 725
2) J. Blons *et al.*, Nucl. Phys. **A414** (1984) 1
3) Yu.B. Ostapenko, G.N. Smirenkin and A.S. Soldatov, Sov. J. Part. Nucl. **12** (1981) 545
4) G. Bellia *et al.*, Z. Phys. **A308** (1982) 149
5) V.E. Zhuchko *et al.*, Sov. J. Nucl. Phys. **28** (1978) 602
6) G. Bellia *et al.*, Phys. Rev. **C24** (1981) 2762
7) J.T. Caldwell and E.J. Dowdy, Nucl. Sci. Eng. **56** (1975) 179
8) J.T. Caldwell *et al.*, Phys. Rev. **C21** (1980) 1215
9) J.T. Caldwell *et al.*, Nucl. Sci. Eng. **73** (1980) 153
10) A.M. Khan and J.W. Knowles, Nucl. Phys. **A179** (1972) 333
11) M.V. Yester, R.A. Anderl and R.C. Morrison, Nucl. Phys. **A206** (1973) 593
12) H.X. Zhang, T.R. Yeh and H. Lancman, Phys. Rev. Lett. **53** (1984) 34
13) P.A. Dickey and P. Axel, Phys. Rev. Lett. **35** (1975) 501
14) J.W. Knowles *et al.*, Phys. Lett. **116B** (1982) 315
15) J.E. Lynn, Contemp. Phys. **21** (1980) 483
16) E.W. Lees, B.H. Patrick and E.M. Bowey, Nucl. Instr. Meth. **171** (1980) 29
17) G. Edwards, D.J.S. Findlay and E.W. Lees, Ann. Nucl. Energy **9** (1982) 127
18) N.P. Hawkes, Ph.D. thesis, Univ. of Birmingham, 1985 (unpublished) and Harwell report AERE R-12075
19) D.J.S. Findlay, Nucl. Instr. Meth. **206** (1983) 507
20) D.J.S. Findlay, Nucl. Instr. Meth. **213** (1983) 353
21) G. Edwards, D.J.S. Findlay and E.W. Lees, Ann. Nucl. Energy **8** (1981) 105
22) P. David *et al.*, Int. Conf. Physics and chemistry of fission, Jülich, 1979, IAEA-SM/241-C6, p. 373
23) J. Trochon *et al.*, Proc. Int. Conf. on Nuclear data for science and technology, Antwerp, 1982, ed. K.H. Böckhoff (Reidel, 1983) p. 733
24) J. Dudek, W. Nazarewicz and A. Faessler, Nucl. Phys. **A412** (1984) 61